

Application of ozone/magnetic graphene oxide for degradation of diazinon pesticide from aqueous solutions

Hossein Arfaeinia^a, Hadi Rezaei^b, Kiomars Sharafi^c, Masoud Moradi^{c,a}, Hasan Pasalari^a, Seyed Enayat Hashemi^{d,*}

^aDepartment of Environmental Health Engineering, School of Public Health, Iran University of Medical Sciences, Tehran, Iran, Tel. +989178844836, email: Arfaeiniah@yahoo.com (H. Arfaeinia), Tel. +989183855991, email: mahfooz60@gmail.com (M. Moradi), Tel. +989178824136, email: kiwan.soleimani@gmail.com (H. Pasalari)

^bHealth Network of Sanandaj, Kurdistan University of Medical Sciences, Sanandaj, Iran, Tel. +989189695420, email: hadi1106@yahoo.com (H. Rezaei)

^cStudent Research Committee, Kermanshah University of Medical Sciences, Kermanshah, Iran, Tel. +989183786151, email: kio.sharafi@gmail.com (K. Sharafi)

^dDepartment of Environmental Health Engineering, faculty of Public Health, Bushehr University of Medical Sciences, Bushehr, Iran, Tel. +987733450134, email: e.hashemi@bpums.ac.ir (S.E. Hashemi)

Received 14 July 2017; Accepted 4 March 2018

ABSTRACT

Diazinon (O, O-diethyl-O-[6-methyl-2-(1-methylethyl)-4-pyrimidinyl] phosphorothioate) is one of the most widely used organophosphorus pesticides that are being increasingly detected in water bodies. However, Diazinon is persistent to conventional biological treatment and sole ozonation with lack of hydroxyl radical. Studies on the effective elimination of Diazinon are still quite sporadic and scarce. In this research magnetic graphene oxide/ ozonation (MGO/O₃) were used to Diazinon removal from aqueous solution. The results of this research indicate that the Diazinon abatement rate was considerably accelerated via the hybrid MGO/O₃ which can generate abundant hydroxyl radical, compared to sole ozonation according to scavenging runs, hydroxyl (·OH) radical was obtained to play a main role in synergistic degradation of Diazinon. All results showed that the MGO/O₃ hybrid system is an efficient and suitable option for the removal of emerging organic contaminants from the aqueous solutions.

Keywords: Hybridization; Magnetic graphene oxide; Ozonation; Diazinon; Aqueous solutions

1. Introduction

Water pollution is a serious environmental issue and threatens the human and ecosystem [1–4]. Pesticides are a type of toxic organic components used in agricultural industry to kill harmful insects. One of the major groups of pesticides are organo phosphorus pesticides (OPPs) which have been for more than 40 years after prohibiting use of organo chlorine pesticides for their persistence in the environment [5]. These substances are widely used for their effectiveness in removing pests and weed. However,

OPPs are toxic materials and their broad uses increase risks to the environment and people [6]. Diazinon is one of the most common OPPs used frequently to control a wide range of sucking and chewing insects and mites on a range of crops, including deciduous fruit trees, citrus fruit, bananas, vegetables, potatoes, beet, sugar cane, coffee, cocoa, tea, tobacco, cotton, and rice [7]. Its molecular formula is C₁₂H₂₁N₂PS, molecular weight is 340.3 and density (at 20°C) is 1.117 g/ml [8]. The main environmental concerns about diazinon's use are killing birds, polluting ground water, and bad effects on aquatic creatures [9]. Diazinon and its impacts on the environment have been surveyed in diverse studies [10]. Diazinon might have a

*Corresponding author.

significant impact on water sources because of high degree of mobility and persistence. World Health Organization (WHO) has classified diazinon as a moderately hazardous class II pesticide [8].

It is therefore essential to find an applicable and environmentally friendly method for removing this harmful and non-biodegradable pesticide from water. There are diverse ways to remove diazinon from aqueous environments including chemical coagulation membrane, rocess and bioremediation, photo catalytic degradation, combined photo-fenton, biological oxidation, aerobic degradation, ozonation, adsorption, etc. [11]. Catalytic ozonation is one of the effective techniques for the removal of toxic materials due to improving the OH \cdot concentration [12]. Many studies have reported the use of carbon based compounds such as graphene oxide (GO), because of its dual role both as an applicable adsorbent and a suitable catalyst which can have interaction with ozone molecules simultaneously and improve the generation of hydroxyl radical for degrading aqueous pollutants. GO consists of a hexagonal rings-based carbon network with a large delocalized electron system and abundance of various oxygen functional groups including –OH, epoxy and carbonyl groups. Furthermore, it also enjoys a high surface area and also delocalized p-p bonding, ideal for electrostatic interactions [13]. These characteristics make GO a water dispersible compound with high attraction toward different substances via diverse interactions (electrostatic interaction, hydrogen bonding and stacking dispersion forces) [14]. Although GO is very advantageous and its efficiency is 10-fold higher than that of other compounds such as carbon active, it has some important disadvantages. Use of GO for adsorption is time-consuming and needs ultra-speed centrifuges [15]. To conquer these deficiencies, magnetic nano composites of Fe₃O₄/GO have been produced. Fe₃O₄/GO has a higher reaction rate than GO and it is very effective in extracting and removing different toxic compounds such as pesticides from water and wastewater. Moreover, Fe₃O₄/GO is quickly and easily extracted from aqueous environments by applying an external magnet [16]. In this study, at first the GO was synthesized by Hummer method. Then, magnetic Fe₃O₄/GO nano composites were produced from GO and were applied for catalytic ozonation of diazinon in aqueous environment.

2. Materials and methods

2.1. Materials

All reagents used in this study were of analytical reagent grade, used deprived of further purification. Graphite powder (100–200 mesh), disodium hydrogen phosphate, iron (III) chloride hexahydrate, monosodium phosphate, sodium nitrate, sulfuric acid, iron (II) chloride tetrahydrate, Tert-butyl alcohol, hydrochloric acid, humic acid, hydrogen peroxide, sodium bicarbonate, and potassium permanganate were obtained from Merck company. Diazinone with 95% purity (technical grade) was purchased from Sigma-Aldrich and used in this work without further purification. Ultra pure water (UPW) was used for making the synthetic samples, with M NaOH and M HCl solutions used for pH adjustment.

2.2. Preparation of graphene oxide (GO) and magnetic graphene oxide (MGO)

GO was synthesized using natural graphite powder and according to the modified Hummer method [17]. Graphite (3 g) and sodium nitrate (3 g) were dissolved into sulfuric acid (140 mL) and the mixture was stirred in cool water. Then, 18 g of potassium permanganate was added to the solution slowly. The temperature of reaction mixture was raised to 40°C and stirred for 60 min. Subsequently, 200 ml of deionized water was added and the temperature was heightened to 90°C for 35 min. Finally, 600 mL of deionized water was added to the solution slowly, which was followed by addition of 20 mL of hydrogen peroxide (30%). The obtained mixture was centrifuged, filtered and washed with M hydrochloric acid 0.1 and water. The deposited GO precipitate was dispersed in 1:5 ratio of water/methanol and centrifuged with three replicate steps at 12000 rpm for 20 min. Eventually, the obtained sample was dissolved in water and then centrifuged at 3000 rpm to produce GO sheets.

To synthesize MGO, initially, 1.8 g of GO dispersion was performed via ultrasound in 500 mL water and sonicated for about 60 min. Then, 0.08 mole of iron (III) chloride hexahydrate and 0.04 mole of iron (II) chloride tetrahydrate were dissolved in 50 mL of water solution, which was added slowly to GO solution at laboratory conditions with 40 mL/min flow of nitrogen and stirred vigorously. After that, for preparing MGO, ammonia solution (28%) was added drop wise to obtain solution pH = 11, the solution temperature was elevated to about 80°C. After being stirred for 4 h, the temperature of mixture was decreased to lab temperature. The prepared MGO was washed thoroughly with UPW and separated by magnetic collection, and finally dried at 100°C under vacuum for 6 h [18].

2.3. Characteristics of prepared magnetic graphene oxide (MGO)

The XRD analysis of MGO was conducted using X-ray diffraction (XRD) method (Philips diffractometer type XPERT) (D8 Advance, Bruker, Germany) with graphite monochromatic copper radiation (Cu K α , $\lambda = 1.54\text{Å}$) at 40 kV, 40 mA, and 25°C. The surface morphology of the powders was analyzed using SEM (MIRA3, Tescan, Czech Republic), at 5 keV. To study the shape and size of the synthesized MGO, TEM (PHILIPS, EM) was used at 100 keV. Magnetization analyses were done with a vibrating sample magnetometer (VSM, 7400, Lakeshore, USA) under magnetic field applied at ambient temperature. Fourier transform infrared spectrophotometer (FTIR) spectra of the MGO composite were obtained using Tensor 27, Bruker, (Germany) to verify the presence of functional groups.

2.4. Adsorption and ozonation procedures and analytical techniques

Adsorption and ozonation were both conducted in a semi-batch reactor at about 25°C and constantly stirred. The effect of various operational factors such as free-radicals, initial pHs, humic acid and bicarbonate on diazinon removal was evaluated. Ozon was produced from purified oxygen (99.8%) by a commercial generator (ARDA, model

AEGCOG-5S) and fed to the solution from the bottom of the reactor. The excess ozone in the off-gas stream was measured by KI titration. In the catalytic ozonation runs, experiments were initiated by feeding ozone into diazinon aqueous solution containing a specific amount of MGO under stirring at 750 rpm. Next, residual concentration of diazinon in the reaction solution was measured by a spectrophotometer (UV/Vis Spectrophotometer, 7400CE CECIL) at $\lambda_{\max} = 300$ nm. All experiments were replicated for three times and the mean values were used in this work.

3. Results and discussion

3.1. Characterization of the catalyst

The X-ray diffraction patterns (XRD) of the GO and MGO are presented in Fig. 1. As shown in this figure, the peak placed at 2θ of 98° is attributed to (001) planes of graphene oxide. Moreover, two weakened peaks at 2θ of 22.06 and 42.38 are related to GO. In comparison with diffraction peak (001) of GO, the peaks of graphene oxide disappeared to a large extent in XRD of MGO at 2θ of 9.98. This phenomenon can be attributed to three reasons including the exfoliation of GO layers, less agglomerate of graphene sheets in the MGO composite and accumulation of strong Fe_3O_4 signals on weak signals of carbon. In addition, the XRD of MGO indicates that the peaks at 2θ of 30, 35, 43, 53, 57 and 62 are attributed to 220, 331, 400, 422, 511 and 440, which is consistent with the standard XRD pattern of the cubic crystalline structures of Fe_3O_4 [19]. The peaks at 2θ of 30, 35, 43, and 57 correspond to magnetite and maghemite, while the peaks at 2θ of 53 and 62 are related to hematite. Overall, the presence of Fe_3O_4 particles in the graphene structure was confirmed XRD analysis, so the prepared catalyst can be separated from water using magnet [20].

Figs. 2 and 3 reveal the FT-IR spectra of GO and MGO nano particles before the adsorption (A) and after the adsorption of diazinon on MGO nano particles' surface (B). As shown in the figures, the peak within the range of 2960

and 1450 $1/\text{cm}$ show asymmetrical C-H stretches, while those located at 2940 and 1375 $1/\text{cm}$ belong to asymmetrical C-H stretches. Moreover, two peaks at 1000 to 1200 $1/\text{cm}$ and bands at 2250 $1/\text{cm}$ are attributed to C-O groups and S-H bonds, respectively. The C=O, Methyl and C=C groups are appeared at 1730, 1380 and 1640 $1/\text{cm}$ peaks, respectively. Other bonds, emerging at 655, 1010, 1100 and 1515 $1/\text{cm}$ are resulted from P-O bonding, C-C stretch bonds and P-S bond [21]. Moreover, the strong adsorption peak at about 570 cm^{-1} in FTIR spectra of MGO is related to Fe-O band, confirming successful synthesis of Fe_3O_4 .

After the runs, the peak located at about 1380 $1/\text{cm}$ disappeared, while two new peaks at 1548 and 1730 $1/\text{cm}$ appeared which can be related to P=S and C=O groups of Diazinon. It was also found from the EDS analysis that S and P were observed after the adsorption of Diazinon (Table 1). Moreover, the peak located at 1010 $1/\text{cm}$ is related to the P-O group; it can be concluded that the sharp peak changes to a wide peak and the location of peak shifts to 1234 and 1355 $1/\text{cm}$ after adsorption by MGO. These phenomena can be due to the interaction of MGO with the p-group in the Diazinon molecules [22].

The energy dispersive spectroscopy (EDS) analysis was conducted to characterize the elemental composition of the

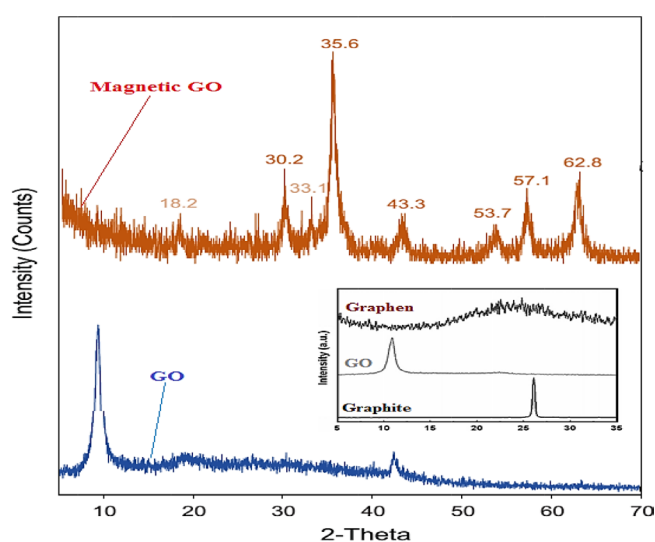


Fig. 1. Typical XRD patterns of samples: GO (Graphene oxide) and MGO (Magnetic graphene oxide).

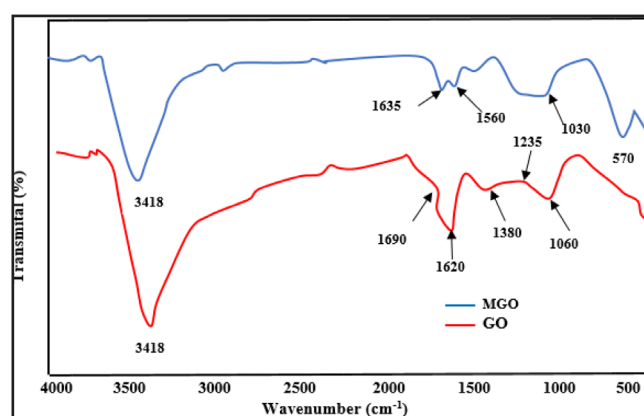


Fig. 2. FTIR image of MGO and GO.

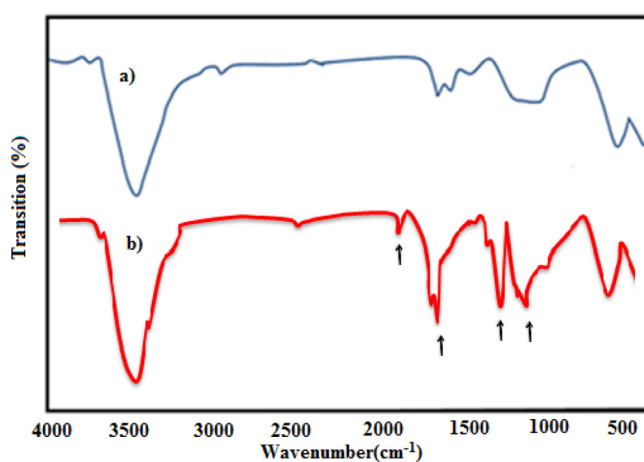


Fig. 3. FTIR image of MGO nano particles before the adsorption (A) and after the adsorption of diazinon on MGO nano particles' surface (B).

Table 1
Elemental composition of MGO after adsorption process

Elements	Atomic weight after adsorption %
Carbon	74.14
Oxygen	9.58
Iron	13.11
Sulfur	2.01
Phosphorus	1.16

MGO composite. As indicated in Fig. 4, the EDS analysis of the MGO sample shows the existence of C, O, and Fe as the main elements, suggesting the grafting of Fe_3O_4 onto GO. Additionally, the SEM image of GO, Fe_3O_4 and MGO composite at 5 keV is demonstrated in Fig. 5. As shown in this figure, the external surface of the composite has irregular cavities. This coarse and uniform surface afford appropriate reactive sites and high reactivity for the composite. This shows that GO sheets can be used as a proper support for the coating of the Fe_3O_4 nano particles. Moreover, magnetic Fe_3O_4 nano par-

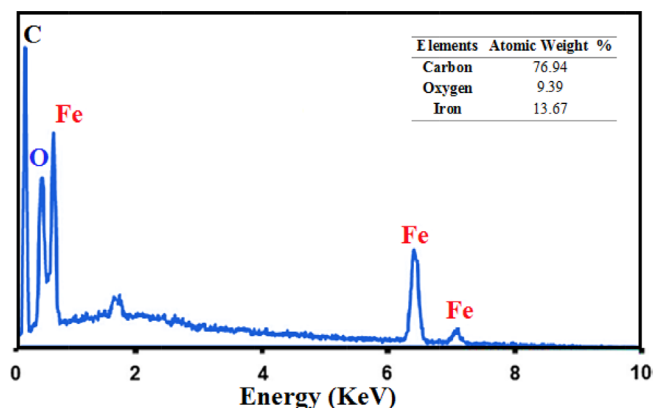


Fig. 4. Typical EDX patterns of MGO.

ticles are closely attached to the surface of graphene, which actually acts as a magnetically inert support at the surface of magnetic layer in the composite, thus influencing the uniformity and magnitude of magnetization [23].

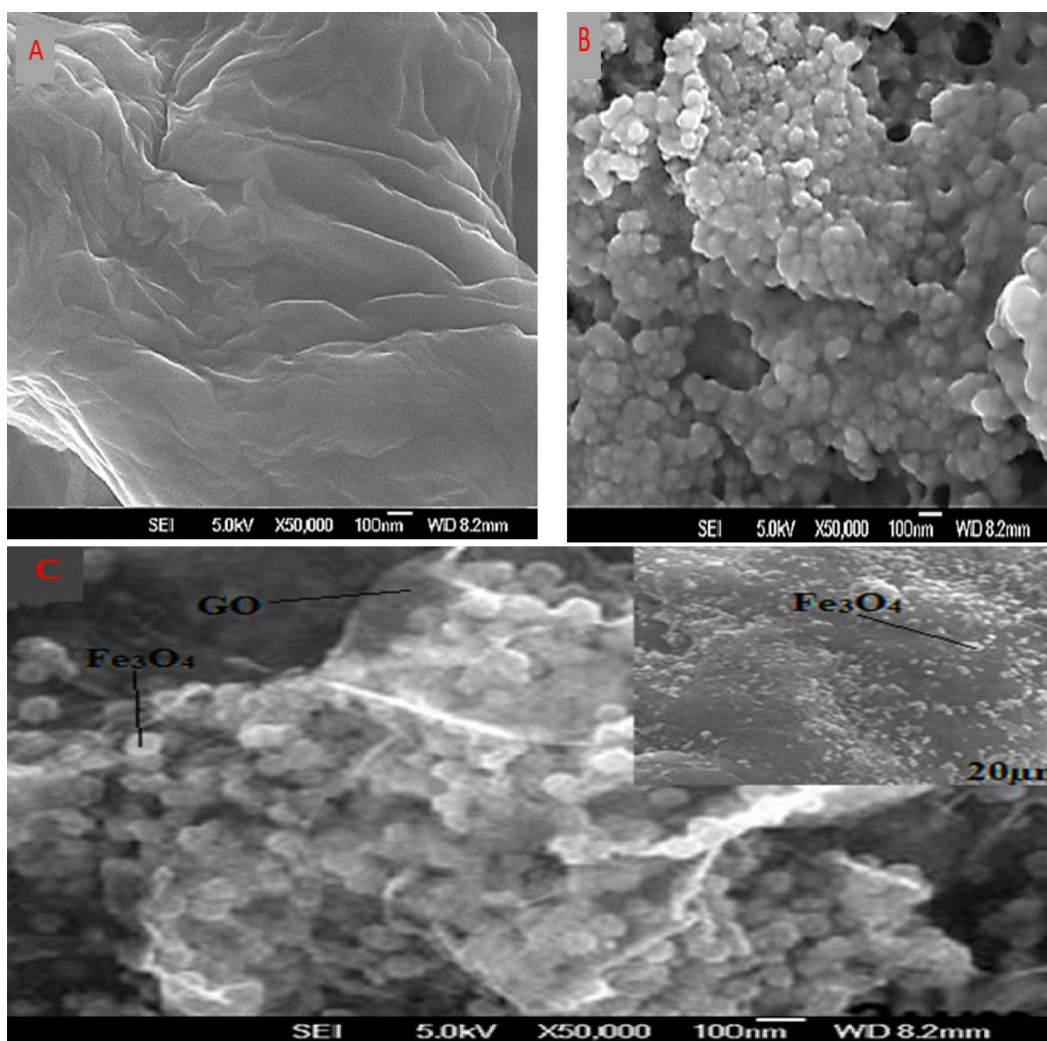


Fig. 5. The SEM images of samples: GO (A), Fe_3O_4 (B) and MGO (C).

TEM analysis was employed to observe the morphology of GO and MGO (Fig. 6). As revealed in TEM images, Fe_3O_4 particles with cubic structure have been coated on the GO surface and aggregated due to their remarkably nanosize and dipole–dipole structure. According to this analysis, successful synthesis of nanosized Fe_3O_4 particles has been confirmed. In this regard, the darkness in the center of the cubic space verified the existence of Fe_3O_4 [24].

The loops of magnetization hysteresis of the Fe_3O_4 and MGO at room temperature are illustrated in Fig. 7. The findings indicated that the magnetization saturation values of Fe_3O_4 and MGO were 47.2 and 38.5 emu/g, respectively, which due to the S curve shows a super paramagnetic characteristic behavior without coercivity and remanence. The lower magnetization value for the MGO composite compared with naked Fe_3O_4 can be owing to the presence of GO (non-magnetic) on the surface of the Fe_3O_4 nano particles [24]. These results confirm that the composite can be potentially used as a magnetic composite to eliminate the pollutants from the aqueous environment without any secondary pollution [25].

3.2. Abatement of diazinon during different process

Changes of Diazinon concentration during sole MGO adsorption influence, sole ozonation influence, ozonation/GO, ozonation/ Fe_3O_4 and ozonation/MGO hybrid influence are presented in Fig. 8. MGO can be used as an adsorbent for adsorption of pollutants and a catalyst for degradation during ozonation process. As seen in Fig. 8a, the elimination of Diazinon during single MGO adsorption at various MGO dosages was very limited, showing that use of MGO as an adsorbent for removal of Diazinon was unfeasible.

With ozonation/GO and ozonation/ Fe_3O_4 , the removal of Diazinon was reached to about 44 and 51% during 9 min, respectively. In ozonation/GO, the degradation of Dia-

zinon can be attributed to the re-oxidization of graphene oxide by O_3 and forming O-GO, which contains more carbonyl and carboxy improving catalytic active of GO [26]. In ozonation/ Fe_3O_4 , the Fe_3O_4 nano particles improved ozone decomposition rate. These nano catalysts can also catalyze Diazinon to generate more Lewis active acid site and ozone was showed strongly bonded with Lewis active acid sites. Thus, the more Lewis active acid sites meant more O_3 molecular being attracted to degrade the Diazinon conveniently, attributing to higher Diazinon removal efficiency [26,27]. Comparatively, in O_3 /MGO process (Fig. 8b), Diazinon concentration was reduced significantly and over 100% of removal efficiency was obtained during 9 min, while the single ozonation process only contributed to about 39% of Diazinon removal. Based on the findings of catalytic ozonation and adsorption runs in this work, the decay of Diazinon was dependent on the degradation of Diazinon, unlike the

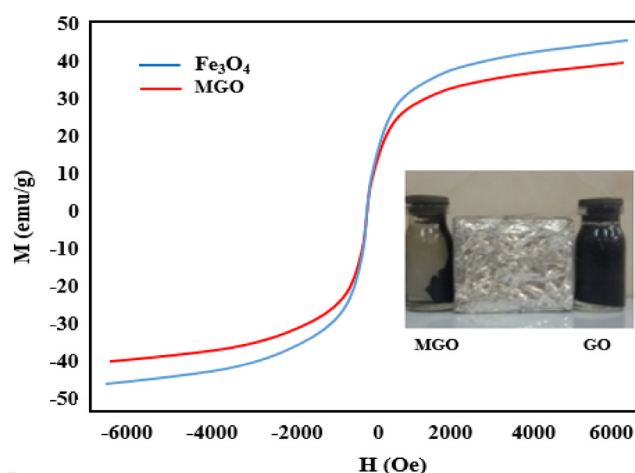


Fig. 7. The magnetization hysteresis loops of Fe_3O_4 and MGO.

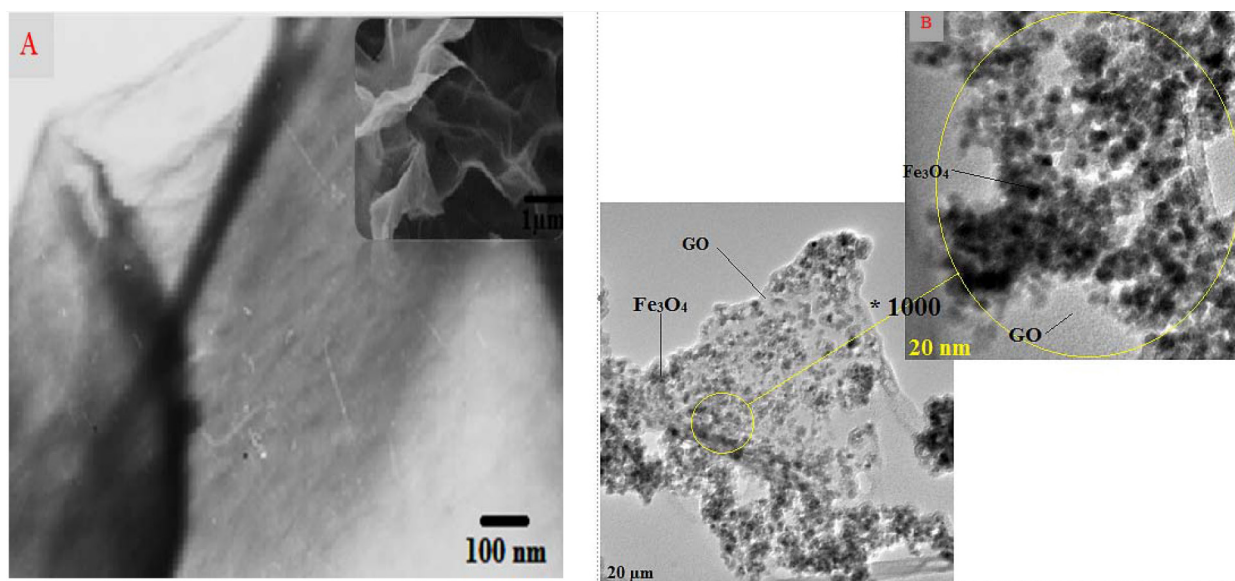


Fig. 6. The TEM of GO (A), MGO (B).

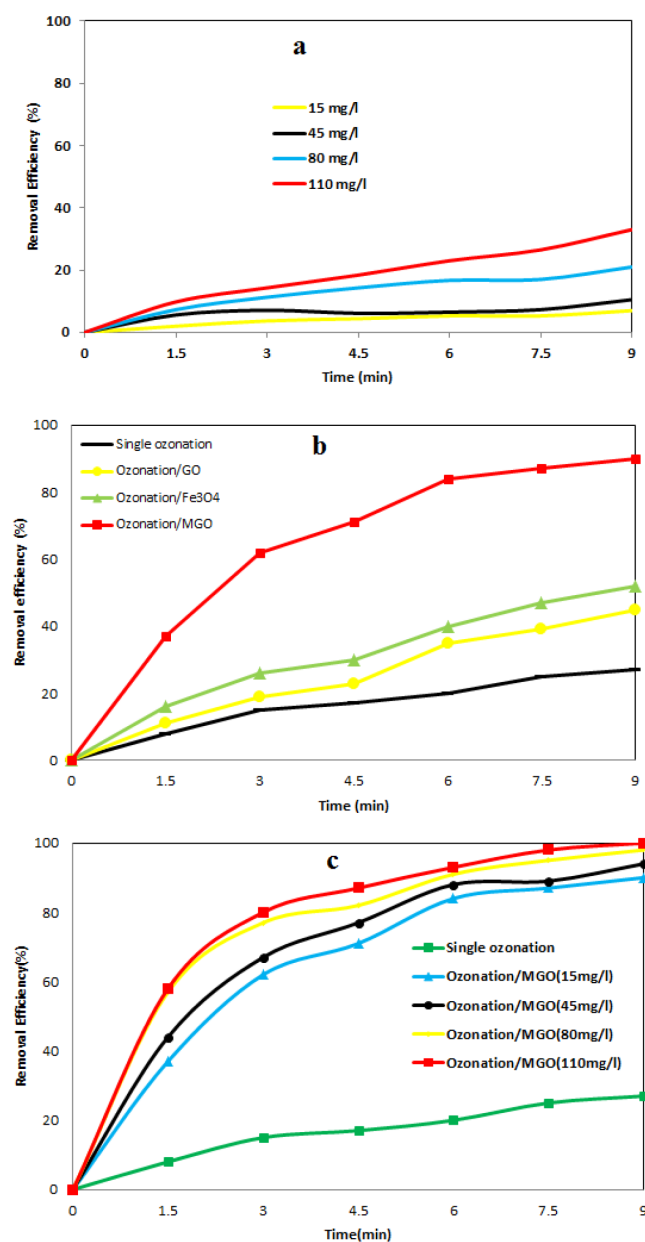


Fig. 8. Diazinon removal with (a) adsorption and (b) catalytic ozonation (MGO/O₃) in a presence of various concentration of MGO, operational conditions: [Diazinon] = 20 mg/L and pH = 7..

previously published paper that iron oxides/multi walled carbon nano tubes which adsorbed pollutant (1-naphthol) on the adsorbent, then degraded it by ozonation [28]. It has been reported that the elimination of pyruvic acid by activated carbon/ozone obtained an elimination efficiency of 90%, compared to about 10% by single ozonation influence [29]. In addition to activated carbon, MWCNTs along with ozonation can also improve the degradation of toxic organic contaminants compared to single ozonation [30]. With elevation of the MGO dosages, the catalytic removal of MGO/O₃ was not improved as much as expected. This shows that it is not an efficient method to enhance the conversion of ozone into hydroxyl radicals via simple addition of MGO.

The similar catalytic removal efficiency at various dosage of MGO showed that MGO powder may prevent the mass transfer process of ozone. Alternatively, excess MGO may inactivate the active species, such as hydroxyl radicals [31].

3.3. The effect of pH on Diazinon removal

Organic contaminants in water solutions with different pH values convert to diverse derivatives [32–34]. Each pollutant possesses different structural features when interacting with O₃ or hydroxyl radicals at unique rate constants [35]. Also, the transformation rate of O₃ molecules could change with pH [36]. Thus, it is necessary to evaluate the effect of pH on Diazinon degradation through MGO/O₃ catalytic system. The degradation of Diazinon by MGO/O₃ at various pH conditions is indicated in Fig. 9. The Diazinon removal declined from 89% to 23% when pH changed from 7 to 3, respectively. Additionally, the degradation rate of Diazinon at alkaline state (pH = 9) was similar to that of the pH = 7 (neutral condition). Theoretically, hydroxyl ions (OH⁻ ion) can improve ozone molecules decomposition into hydroxyl radicals, so that the degradation rate of the model pollutants could be largely intensified by the raise of pH values [37]. However, when pH rose from 7 to 9, the enhancing influence was not significant. As reported by a previously published paper [38], in buffered status of water, the k_{obs2} of organic pollutant increase with rising pH, and then it declined when the pH exceeds the threshold. This may be due to formation of high levels of hydroxyl ions (OH⁻ ion), leading to ozone instability in water, causing in lowered of dissolved ozone [39].

3.4. The influence of EDTA on diazinon elimination

In this study, a few runs were conducted to measure the effect of EDTA (as a model of natural organic matter) to evaluate the interaction between dissolved organic matters (DOM) and MGO/O₃ process. As indicated in Fig. 10, the addition of EDTA (0.4 mg-C/L and 4 mg-C/L) led to non-significant changes, but just a slight prevention of the degradation of Diazinon. However, with the addition of EDTA by up to g mg-C/L, the removal of the combined MGO/O₃ process was not affected. This finding is consistent with the results obtained in a study where MWCNTs/ozonation hybrid was used for removing organic matters [30]. In another study where the influence of humic acid (HA) on abatement of cumene and ibuprofen was evaluated with catalytic ozonation, it was observed that the catalysts (ZSM-5 zeolites and γ -alumina) had a low adsorption efficiency towards HA. The catalytic activity was not affected by HA, while HA could inhibit the catalyst production of \cdot OH radicals [40,41]. Thus, it is logical to believe that MGO is hard to adsorb HA on its pores and sites.

3.5. The influence of bicarbonate on diazinon elimination

Other agents that can react with hydroxyl radicals and reduce the removal efficiency of MGO/ozone process are carbonate (CO₃²⁻) and bicarbonate (HCO₃⁻). The second rate constants of CO₃²⁻ and HCO₃⁻ for reaction with \cdot OH are 3.9×10^8 and 8.5×10^6 M⁻¹·s⁻¹, respectively [42]. Under neu-

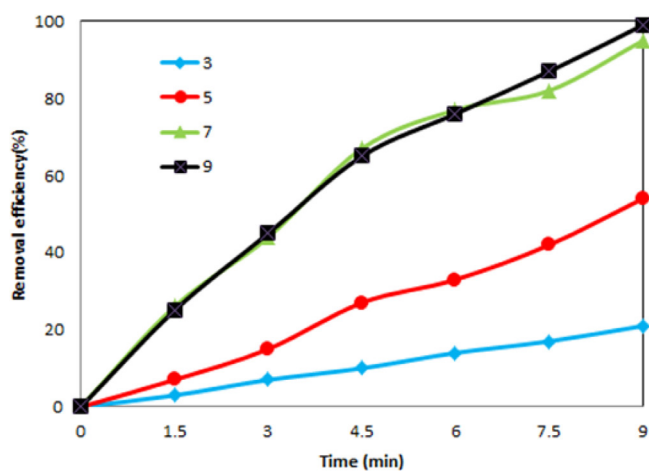


Fig. 9. The effect of various pH on the removal of diazinon, operational conditions: [Diazinon] = 20 mg/L and [MGO] = 15 mg/L.

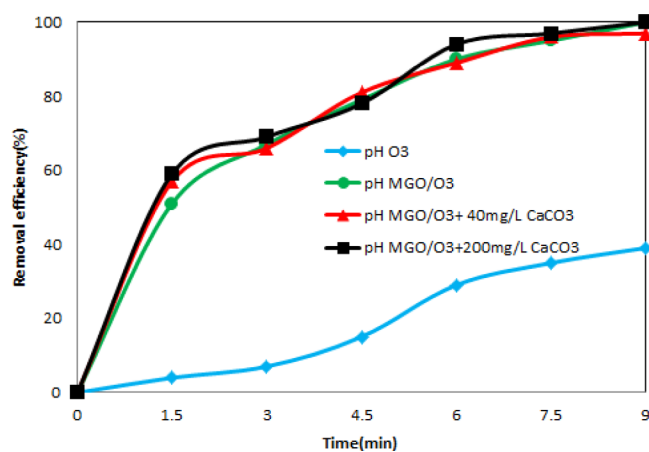


Fig. 11. The removal of Diazinon in the presence of HCO_3^- , operational conditions: [Diazinon] = 20 mg/L, [MGO] = 15 mg/L and pH = 7.

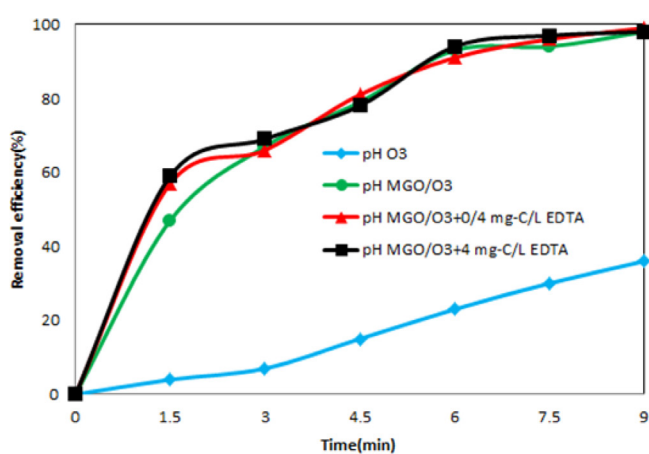


Fig. 10. The removal of diazinon in the presence of EDTA, operational conditions: [Diazinon] = 20 mg/L, [MGO] = 15 mg/L and pH=7.

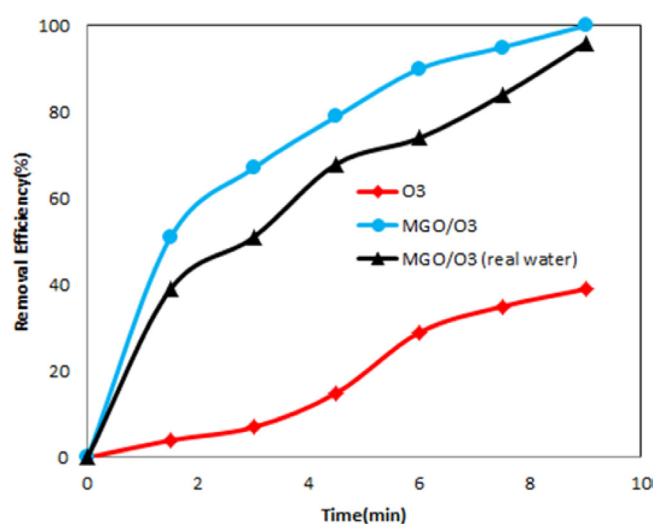


Fig. 12. Normalized Diazinon concentration as a function of contact time in real water, operational conditions: [Diazinon] = 20 mg/L, [MGO] = 15 mg/L and pH=7.

tral conditions, inorganic carbon converts to bicarbonate ion easily, and therefore the bicarbonate is a major form of inorganic carbon in solutions with neutral conditions. As revealed in Fig. 11, the elimination rate of diazinon in the presence of HCO_3^- is slightly lower than the time when the bicarbonate concentration is zero. Moreover, the Diazinon removal efficiency via ozonation was not significantly changed with the rise of carbonate concentrations. A slight difference was also found between the existence and lack of bicarbonate by Jia-Nan et al. for the removal of N, N-diethyl-mtoluamide (DEET) by ozone and carbon-based catalysts. From a theoretical perspective, the abatement rate of model pollutant primarily according to $\cdot\text{OH}$ radicals should have low rate with the addition of bicarbonate as a free radical scavenger. In another research, it has been found that the degradation of nitrobenzene increased first and declined subsequently in the presence of bicarbonate (with increasing from 0 to 200 mg/L) in either the hybrid systems of O_3 /ceramic or O_3 /Mn-ceramic [43].

3.6. The influence of constituents in real water on diazinon elimination

In the final step of this study, an experiment was conducted in real water to confirm the feasibility of MGO/ozone hybrid system in real water bodies. The real water was spiked with diazinon. Simultaneously, deionized water with diazinon was tested under the same condition for comparison. Fig. 12 show indicates that the existence of constituents in real water can quench the removal of diazinon with MGO/ozone hybrid process. It is noteworthy that even there are various constituents in real water; the influence of catalytic activity is significant in comparison with the two waters with different quality status. Thus, an appreciable synergistic effect of MGO and O_3 generating $\cdot\text{OH}$ radicals can contribute to the abatement of diazinon. The results of this research were closely consistent with those reported for reaction kinetics of

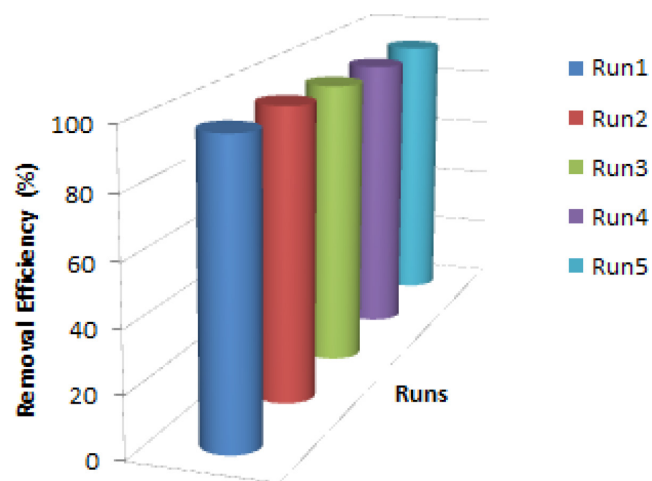


Fig. 13. Reusability of the MGO catalyst in degradation of diazinon pesticide by photo catalytic ozonation.

some micro pollutants in hybrid ozonation (ozone/hydrogen peroxide). It verified that advanced oxidation process (AOPs) depended on hydroxyl radicals is an efficient process to remove target pollutants. The phenomenon is related to the feature of non-selective $\cdot\text{OH}$ radicals [44].

3.7. Stability and reusability of the MGO catalyst

Given that the stability, reuse, and regeneration ability of a typical catalyst are principal factors in its practical application, stability of the MGO catalyst. The findings of five repeated removal runs have been depicted in Fig. 13. It manifests that, after degradation with five runs, the catalytic ability of the MGO declined for each new cycle (96.4 to 92.7%). These results indicate that the MGO can potentially be employed as a magnetic catalyst to degrade pesticide pollutants from water.

4. Conclusion

This research indicated that MGO/ozone hybrid process can be employed as a novel and promising technology, thanks to demonstrating considerable performance relating to diazinon abatement and elimination. In particular, the hybridization of MGO and ozone can remarkably accelerate diazinon removal, while adsorption of diazinon on MGO is limited. These findings can be related to the fact that through MGO/ozonation, $\cdot\text{OH}$ radical is generated and causes synergistic degradation of diazinon. This research also assessed the removal of diazinon with MGO/ozone hybrid process in real conditions. The elimination of diazinon is considerably inhibited under low pH (acidic conditions), showing that hydroxyl radical is suppressed at acidic conditions. The constituents in real water can inhibit the removal of diazinon, while the influences of bicarbonate and HA on diazinon elimination are limited. Generally, this work showed that the MGO and ozonation hybrid technology can be used as a viable method for degrading emerging and toxic organic pollutants in real water bodies.

Disclosure statement

No potential conflict of interest was reported by the authors.

Acknowledgment

The study was financially supported by the research fund provided by the Bushehr University of Medical Sciences, Bushehr, Iran (Grant No: **dp/20/71/91116**). The authors gratefully acknowledge them for assist and support of this work.

References

- [1] M. Moradi, M. Soltanian, M. Pirsaeheb, K. Sharafi, S. Soltanian, A. Mozafari, The efficiency study of pumice powder to lead removal from the aquatic environment: isotherms and kinetics of the reaction, *J. Mazandaran Univ. Med. Sci.*, 23 (2014) 65–75.
- [2] M. Pirsaeheb, T. Khodadadi, Z. Bonyadi, K. Sharafi, T. Khosravi, Evaluation of pesticide residues 2, 4-D, atrazine and alachlor concentration in drinking water well of Mahidasht district-Kermanshah, Iran, 2010–2011. *World Appl Sci J.*, 23 (2013) 1530–1537.
- [3] K. Sharafi, A.M. Mansouri, A.A. Zinatizadeh, M. Pirsaeheb, Adsorptive removal of methylene blue from aqueous solutions by pumice powder: process modelling and kinetic evaluation, *Environ. Eng. Manage. J.*, 14 (2015) 1067–1078.
- [4] V.N. Karbasdehi, S. Dobaradaran, I. Nabipour, H. Arfaeina, R. Mirahmadi, M. Keshtkar, Data on metal contents (As, Ag, Sr, Sn, Sb, and Mo) in sediments and shells of *Trachycardium lacunosum* in the northern part of the Persian Gulf, *Data in Brief*, 8 (2016) 966–971.
- [5] F. Ahmadi, Y. Assadi, S.M. Hosseini, M. Rezaee, Determination of organo phosphorus pesticides in water samples by single drop micro extraction and gas chromatography-flame photo metric detector, *J. Chromatogra. A.*, 1101 (2006) 307–312.
- [6] J. Ye, M. Zhao, J. Liu, W. Liu, Enantios electivity in environmental risk assessment of modern chiral pesticides, *Environ. Pollut.* 158 (2010) 2371–2383.
- [7] V. Sakkas, A. Dimou, K. Pitarakis, G. Mantis, T. Albanis-TiO₂ photo catalyzed degradation of diazinon in an aqueous medium, *Environ. Chem. Lett.*, 3 (2005) 57–61.
- [8] Y. Zhang, Y. Hou, F. Chen, Z. Xiao, J. Zhang, X. Hu, The degradation of chlorpyrifos and diazinon in aqueous solution by ultrasonic irradiation: effect of parameters and degradation pathway, *Chemosphere*, 82 (2011) 1109–1115.
- [9] P. Mineau, M. Whiteside, Lethal risk to birds from insecticide use in the United States—a spatial and temporal analysis, *Environ. Toxicol. Chem.*, 25 (2006) 1214–1222.
- [10] M. Banaee, A. Sureda, A. Mirvaghefi, K. Ahmadi, Effects of diazinon on biochemical parameters of blood in rainbow trout (*Oncorhynchus mykiss*), *Pestic Biochem. Phys.*, 99 (2011) 1–6.
- [11] M. Cycoń, M. Wójcik, Z. Piotrowska-Seget, Biodegradation of the organo phosphorus insecticide diazinon by *Serratia* sp. and *Pseudomonas* sp. and their use in bioremediation of contaminated soil, *Chemosphere*, 76 (2009) 494–501.
- [12] H. Arfaeina, K. Sharafi, S. Banafshehafshan, S.E. Hashemi. degradation and bio degradability enhancement of Chloramphenicol and Azithromycin in aqueous solution using heterogeneous catalytic ozonation in the presence of MgO nano crystal in comparison with single ozonation, *Int. J. Pharm. Tech.*, 8 (2016) 10932–10949.
- [13] D.R. Dreyer, S. Park, C.W. Bielawski, R.S. Ruoff. The chemistry of graphene oxide, *Chem. Soc. Rev.*, 39 (2010) 228–240.
- [14] Q. Liu, J. Shi, J. Sun, T. Wang, L. Zeng, G. Jiang, Graphene and graphene oxide sheets supported on silica as versatile and high-performance adsorbents for solid-phase extraction, *Angew. Chem.*, 123 (2011) 6035–6039.

- [15] B. Kakavandi, A. Jonidi, R. Rezaei, S. Nasserli, A. Ameri, A. Esrafil, Synthesis and properties of Fe_3O_4 -activated carbon magnetic nano particles for removal of aniline from aqueous solution: equilibrium, kinetic and thermodynamic studies, *Iran J. Environ. H. Sci. Eng.*, 10 (2013) 19.
- [16] W. Zhang, X. Shi, Y. Zhang, W. Gu, B. Li, Y. Xian, Synthesis of water-soluble magnetic graphene nano composites for recyclable removal of heavy metal ions, *J. Mater. Chem. A.*, 1 (2013) 1745–1753.
- [17] D.A. Dikin, S. Stankovich, E.J. Zimney, R.D. Piner, G.H. Dommett, G. Evmenenko, et al. Preparation and characterization of graphene oxide paper, *Nature*. 448 (2007) 457–460.
- [18] Y. Yao, S. Miao, S. Liu, L.P. Ma, H. Sun, S. Wang, Synthesis, characterization, and adsorption properties of magnetic Fe_3O_4 @graphene nano composite, *Chem Eng J.*, 184 (2012) 326–332.
- [19] H. Sun, L. Cao, L. Lu, Magnetite/reduced graphene oxide nano composites: one step solvothermal synthesis and use as a novel platform for removal of dye pollutants, *Nano Res.*, 4 (2011) 550–562.
- [20] A. Mohseni-Bandpi, B. Kakavandi, R.R. Kalantary, A. Azari, A. Keramati, Development of a novel magnetite–chitosan composite for the removal of fluoride from drinking water: adsorption modeling and optimization, *Rsc Adv.*, 5 (2015) 73279–73289.
- [21] H. Sereshti, S. Samadi, S. Asgari, M. Karimi. Preparation and application of magnetic graphene oxide coated with a modified chitosan pH-sensitive hydrogel: an efficient biocompatible adsorbent for catechin, *Rsc Adv.*, 5 (2015) 9396–9404.
- [22] J. Hur, J. Shin, J. Yoo, Y.-S. Seo. Competitive adsorption of metals onto magnetic graphene oxide: comparison with other carbonaceous adsorbents, *Scientific World J.*, 2015 (2015).
- [23] H. Wang, X. Yuan, Y. Wu, X. Chen, L. Leng, H. Wang, et al. Facile synthesis of polypyrrole decorated reduced graphene oxide– Fe_3O_4 magnetic composites and its application for the Cr (VI) removal, *Chem Eng J.*, 262 (2015) 597–606.
- [24] X. Zhu, Z. Mo, C. Zhang, B. Wang, G. Zhao, R. Guo, Preparation of graphene- Fe_3O_4 nano composites using Fe^{3+} ion-containing magnetic ionic liquid, *Mater Res Bull.*, 59 (2014) 223–226.
- [25] R.R. Kalantary, A. Azari, A. Esrafil, K. Yaghmaeian, M. Moradi, K. Sharafi. The survey of malathion removal using magnetic graphene oxide nano composite as a novel adsorbent: thermodynamics, isotherms, and kinetic study, *Desal. Water Treat.*, 57 (2016) 28460–28473.
- [26] A. Lv, C. Hu, Y. Nie, J. Qu. Catalytic ozonation of toxic pollutants over magnetic cobalt and manganese co-doped $\gamma\text{-Fe}_2\text{O}_3$, *Appl. Catal. B: Environ.*, 100 (2010) 62–67.
- [27] A. Lv, C. Hu, Y. Nie, J. Qu. Catalytic ozonation of toxic pollutants over magnetic cobalt-doped Fe_3O_4 suspensions, *Appl. Catal. B: Environ.*, 117 (2012) 246–252.
- [28] X. Wang, C. Chen, J. Li, X. Wang, Ozone degradation of 1-naphthol on multi walled carbon nano tubes/iron oxides and recycling of the adsorbent, *Chem. Eng. J.*, 262 (2015) 1303–1310.
- [29] F. Beltrán, B. Acedo, F. Rivas, O. Gimeno, Pyruvic acid removal from water by the simultaneous action of ozone and activated carbon, *Ozone Sci. Eng.*, 27 (2005) 159–169.
- [30] R. Oulton, J.P. Haase, S. Kaalberg, C.T. Redmond, M.J. Nalbandian, D.M. Cwiertny, Hydroxyl radical formation during ozonation of multi walled carbon nanotubes: performance optimization and demonstration of a reactive CNT filter, *Environ Sci Technol.*, 49 (2015) 3687–3697.
- [31] J.-N. Liu, Z. Chen, Q.-Y. Wu, A. Li, H.-Y. Hu, C. Yang. Ozone/graphene oxide catalytic oxidation: a novel method to degrade emerging organic contaminant N, N-diethyl-m-toluamide (DEET), *Scientific Reports*, 6 (2016).
- [32] A. Raeisi, H. Arfaeinia, M. Seifi, M. Shirzad-Siboni, M. Keshtkar, S. Dobaradaran, Polycyclic aromatic hydrocarbons (PAHs) in coastal sediments from urban and industrial areas of Asaluyeh Harbor, Iran: distribution, potential source and ecological risk assessment, *Water Sci Technol.*, 74 (2016) 957–973.
- [33] H. Arfaeinia, B. Ramavandi, K. Sharafi, S. Hashemi, Reductive degradation of ciprofloxacin in aqueous using nano scale zero valent iron modified by Mg-aminoclay, *Int. J. Pharm. Tech.*, 8 (2016) 13125–13136.
- [34] M. Pirsaeheb, Z. Rezai, A.M. Mansouri, A. Rastegar, A. Alahabadi, A.R. Sani, K. Sharafi, Preparation of the activated carbon from India shrub wood and their application for methylene blue removal: modeling and optimization, *Desal. Water Treat.*, 57 (2016) 5888–5902.
- [35] X. Jin, S. Peldszus, P.M. Huck, Reaction kinetics of selected micro pollutants in ozonation and advanced oxidation processes, *Water Res.*, 46 (2012) 6519–6530.
- [36] Y. Guo, B. Xu, F. Qi, A novel ceramic membrane coated with $\text{MnO}_2\text{-Co}_3\text{O}_4$ nano particles catalytic ozonation for benzophenone-3 degradation in aqueous solution: Fabrication, characterization and performance, *Chem. Eng. J.*, 287 (2016) 381–389.
- [37] L. Yuan, J. Shen, Z. Chen, X. Guan, Role of Fe/pumice composition and structure in promoting ozonation reactions, *Appl Catal B-Environ.*, 180 (2016) 707–714.
- [38] K.S. Tay, N.A. Rahman, M.R.B. Abas, Degradation of DEET by ozonation in aqueous solution, *Chemosphere*, 76 (2009) 1296–302.
- [39] H.-F. Miao, M. Cao, D.-Y. Xu, H.-Y. Ren, M.-X. Zhao, Z.-X. Huang, et al. Degradation of phenazone in aqueous solution with ozone: Influencing factors and degradation pathways, *Chemosphere*, 119 (2015) 326–333.
- [40] A. Ikhlaq, D.R. Brown, B. Kasprzyk-Hordern. Catalytic ozonation for the removal of organic contaminants in water on alumina, *Appl Catal. B-Environ.*, 165 (2015) 408–418.
- [41] M. Karimaei, K. Sharafi, M. Moradi, H.R. Ghaffari, H. Biglari, H. Arfaeinia, et al. Optimization of a methodology for simultaneous determination of twelve chlorophenols in environmental water samples using in situ derivatization and continuous sample drop flow micro extraction combined with gas chromatography-electron-capture detection, *Anal Method*, 9 (2017) 2865–2872.
- [42] G.V. Buxton, C.L. Greenstock, W.P. Helman, A.B. Ross, Critical review of rate constants for reactions of hydrated electrons, hydrogen atoms and hydroxyl radicals ($\cdot\text{OH}/\cdot\text{O}^-$ in aqueous solution), *J. Phys. Chem. Ref. data*, 17 (1988) 513–886.
- [43] L. Zhao, Z. Sun, J. Ma, H. Liu, Influencing mechanism of bicarbonate on the catalytic ozonation of nitrobenzene in aqueous solution by ceramic honeycomb supported manganese, *J. Mol Catal A-Chem.*, 322 (2010) 26–32.
- [44] Y. Yang, J. Jiang, X. Lu, J. Ma, Y. Liu, Production of sulfate radical and hydroxyl radical by reaction of ozone with peroxy-mono sulfate: a novel advanced oxidation process, *Environ Sci. Technol.*, 49 (2015) 733–739.